# Circumventing the pathological behavior of path-integral Monte Carlo for systems with Coulomb potentials

M. H. Müser and B. J. Berne
*Department of Chemistry, Columbia University, New York, New York 10027*

(Received 29 January 1997; accepted 18 March 1997)

The imaginary-time discretized path integral for systems interacting through Coulomb potentials and/or bounded by hard walls behaves pathologically. In this paper we give an analysis of the pathologies. A new method is used to calculate the path integral for the Coulomb system within the primitive algorithm. This is done by constructing an effective potential that implicitly depends on Trotter number $P$. The procedure makes possible the treatment of Coulombic potentials by means of Monte Carlo at surprisingly low Trotter numbers and without the need of computing three-body potentials, necessary when high-order approximants for the density matrix are employed. © *1997 American Institute of Physics.* [S0021-9606(97)50324-2]

## I. INTRODUCTION

Path-integral Monte Carlo (PIMC) techniques have been used to treat multi-particle systems. Using a discretized version of the Feynman path integral for the canonical density matrix, $\rho(\beta)$, the canonical partition function for an $N$-particle quantum system can be shown to be isomorphic to the partition function, $Z_P(\beta)$, for an $N\times P$ particle classical system with $P$ being the number of time slices in the discretization, sometimes called the Trotter number. Standard Monte Carlo techniques can then be applied to study the isomorphic classical system. $Z_P(\beta)$ obeys[1]

$$Z(\beta)=Z_P(\beta)+\mathcal{O}\left(\frac{\beta^2}{P^2}\langle[T_{\rm kin},V]\rangle\right), \tag{1}$$

with $[T_{\rm kin},V]$ the commutator of kinetic and potential energy and thus $Z_P(\beta)$ converges to the quantum limit with $P^{-2}$.

There are, however, pathological systems for which the thermal average $\langle[T_{\rm kin},V]\rangle$ is not defined, making standard techniques to extrapolate from finite $P$ data to the quantum limit unemployable. It is convenient to further distinguish between systems which still yield the right quantum limit for large $P$, e.g., with $P^{-\nu}$ and $0<\nu<2$, and systems where the quantum limit can not be obtained at all by the method outlined above, usually being referred to as the primitive algorithm. We call these systems ''weakly'' and ''strongly'' pathological for the primitive path-integral Monte Carlo scheme, respectively.

Examples of weakly pathological systems are systems interacting through hard-sphere interactions or particles surrounded by hard walls. The treatment of those models in the framework of PIMC simulation was originally addressed by Barker[2] for particles in a (cubic) box and by Jacucci and Omerti[3] for particles in a spherical cavity. We provide a brief summary here to show how observables such as internal energy and (thermal) probability density scale *quantitatively* to the quantum limit for both the primitive algorithm and the so-called image approximation.

Of greater importance is the treatment of the strongly pathological attractive Coulomb potential. It is well known that the path generated by PIMC simulations collapses into $r=0$ if the primitive algorithm is employed.[4] The collapse into $r=0$ can be circumvented if high-order approximants[5] for $\rho(\beta)$ are employed. Li and Broughton were the first to apply such a high-order approximant, the Takahashi–Imada approximant,[6] to the Coulomb potential.[7] They report not completely satisfactory results. At temperatures $T=3150$ K and Trotter numbers as high as $P=800$ the agreement in the radial distribution function of the $(1s)$ electron in hydrogen between simulation and exact theory is still poor. Even though for well-behaved potentials the systematic error in $Z(\beta)$ vanishes proportionally to $\mathcal{O}(P^{-4})$ in the Takahashi–Imada algorithm,[6] Li and Broughton estimate that the error cannot decrease faster than $\mathcal{O}(P^{-1/2})$. This arises from the fact that in the Takahashi–Imada algorithm an effective potential is constructed that is repulsive at short distances $r$ and that becomes proportional to $r^{-4}$ for both attractive and repulsive Coulomb potentials. Consequently the probability density or the distribution function $g(r)/r^2$ at $r=0$ will always be zero, independent of $P$. Hence the Coulomb potential is still weakly pathological in terms of high-order approximant PIMC simulation and if we take $\lim_{r\to 0}g(r)/r^2$ as the relevant observable, it even remains strongly pathological.

Despite the title ''Path-integral simulation of positronium in a hard sphere,'' Ref. 8 is not based on the standard path-integral algorithm. An **S** partial wave matrix-squaring method has been used in order to avoid the collapse into $r=0$. Such an approach, however, is only suitable for low-dimensional systems and highly symmetric boundary conditions such as spherical cavities. Hence this approach does not have the advantages of the standard PIMC scheme for which the computational effort increases linearly with particle number and for which an increase in the complexity of the problem does not increase the computational effort unless the system slows down due to frustration. Similarly, the PIMC simulation of the hydrogen plasma,[9] where the high-temperature density matrix has been obtained by a pair-product approximation, does not have all the advantages the primitive algorithm *usually* has.

The basic idea invoked in this paper is to make Coulom-

bic potentials accessible to PIMC by simulating an effective potential $V_{\rm eff}(r,a)$ instead of the Coulomb potential $V_{\rm C}(r)$ itself, where $V_{\rm eff}(r,a)$ does not have a singularity but tends to $V_{\rm C}(r)$ as the ''damping radius'' $a\to 0$. Then the partition function[10] can be obtained by

$$Z(\beta)=\lim_{a\to 0}\lim_{P\to\infty}\mathrm{Tr}[e^{-\beta T_{\rm kin}/P}e^{-\beta V_{\rm eff}(a,r)/P}]^P \tag{2}$$

$$\neq \lim_{P\to\infty}\lim_{a\to 0}\mathrm{Tr}[e^{-\beta T_{\rm kin}/P}e^{-\beta V_{\rm eff}(a,r)/P}]^P. \tag{3}$$

The effective potential should have the following two properties in addition: (i) for large $r$ it should converge at least exponentially fast to $V_{\rm C}$. (ii) Ewald summations for periodically repeated systems should still be possible. The following effective potential shows these features:

$$V_{\rm eff}(r,a)=-\frac{1}{4\pi\varepsilon_0}\frac{e^2}{r}(1-e^{-r/a}). \tag{4}$$

It is well-behaved, bounded from below and from above. Hence $\langle[T_{\rm kin},V_{\rm eff}]\rangle$ exists for $a>0$ and $V_{\rm eff}$ is not pathological in terms of the primitive algorithm. It is of course desirable to let $a\to 0$ simultaneously as $P$ goes to infinity, but it has to be done such that Eq. (2) holds. In this paper, we will show that $a\propto P^{-2/3}$ is the optimal choice for the primitive algorithm. This approach for treating Coulmbic potentials will not only be useful for PIMC simulation but also for diagonalization techniques of high-temperature density matrices.

The effective Coulomb potential method, presented in this paper, does not treat the sign problem,[11,12] which arises from the fermionic character of the electrons. This is a different topic that must be solved before this approach will be fully effective. However, as long as exchange can be neglected, e.g., in a hot electronic plasma, or as long as there are only two indistinguishable fermions, e.g., dissociation of an $H_2$-molecule in solution, the above approach makes possible the efficient application of PIMC to these problems.

## II. HARD WALLS

### A. Theory

In this section we show why the particle-in-a-box problem is weakly pathological and moreover how the use of the image approximation of Barker removes the weak pathology. Usually the discretized version of a (real-time) path-integral yields reasonable results if for ''typical'' paths the inequality,

$$|V(x_t)-V(x_{t+1})|\ll\left|\frac{m(x_t-x_{t+1})^2}{2\Delta t^2}\right|, \tag{5}$$

holds. For imaginary-time paths, on which PIMC is based, a similar condition must be satisfied by the replacement $t\to -i\beta\hbar$. Clearly this condition can not be met when infinitely high walls are present as formally expressed in the following Hamiltonian:

$$H=\frac{p^2}{2m}+\lim_{V_0\to\infty}V_0\Theta\left(\frac{d}{2}-\left|x\right|\right), \tag{6}$$

where $d$ is the length of the box. The condition, Eq. (5), can alternatively be formulated by

$$|\langle\psi_{\rm t}|[T_{\rm kin},V]|\psi_{\rm t}\rangle|\ll\frac{\beta^2}{P^2}, \tag{7}$$

with $\psi_{\rm t}$ the thermal wavefunction, $\psi_t(x)=\Sigma_n\exp[-\beta H/2]|{\rm n}\rangle$. This expression is easy to calculate analytically at zero temperatures for finite $V_0$

$$\lim_{T\to 0}\langle[T_{\rm kin},V]|\rangle=-\frac{\hbar^2}{m}\mathscr{R}e\int dx\left(\frac{\partial}{\partial x}\psi_0^*\right)\left(\frac{\partial}{\partial x}V\right)\psi_0 \tag{8}$$

$$=-\frac{\pi\hbar^3\sqrt{V_0}}{a^3\sqrt{32m^3}}+\mathscr{O}(V_0^0), \tag{9}$$

since the groundstate $\psi_0$ corresponds at $T=0$ to the thermal wavefunction. It is an easy matter to see that the singularity, proportional to $\sqrt{V_0}$ in Eq. (8), also holds if the bracket on the right-hand side of Eq. (8) is evaluated with any arbitrary (bounded) eigenfunction. Hence at finite temperatures one obtains

$$\langle[T_{\rm kin},V]\rangle\propto\sqrt{V_0}. \tag{10}$$

This means that the partition function[13] and hence most observables can not be expressed as an analytic function of $P^2$ in a path-integral approach. A simple argument, however, shows that the partition function approaches the correct quantum limit as $P^{-1/2}$. For infinite $P$ the partition function is an analytic function of only one parameter, namely $\beta E_1$. For finite $P$ an extra parameter comes into play, the de Broglie wavelength $\lambda(\beta/P)$ at the reciprocal temperature $\tilde{T}^{-1}=\beta/Pk_{\rm B}$. Hence the partition function depends on $\beta E_1$ and $\lambda(\beta/P)/d$. This dependence is (for obvious reasons) again analytic and hence the first correction term to the quantum-limit goes as $\lambda(\beta/P)/d$; that is, as $P^{-1/2}$.

Since the eigenfunctions $\psi_n$ of the ''particle-in-a-box'' problem are well known the *exact* free-particle density matrix (or propagator) can easily be calculated by[2]

$$\rho\left(x,x';\frac{\beta}{P}\right)=\sum_n\psi_n(x)\psi_n(x')e^{-\beta E_n/P}, \tag{11}$$

$E_n=\hbar^2\pi^2n^2/2md^2$ being the eigenenergies. With the help of a Poisson formula this sum can be reexpressed as

$$\rho\left(x,x';\frac{\beta}{P}\right)=\frac{1}{\lambda(\beta/P)}\sum_{\nu=-\infty}^{\infty}(-1)^\nu\theta\left(\frac{d}{2}-|x|\right)\theta\left(\frac{d}{2}-|x'|\right)\times\exp\left[-\frac{mP}{2\beta\hbar^2}\{\nu d+x+(-1)^\nu x'\}^2\right], \tag{12}$$

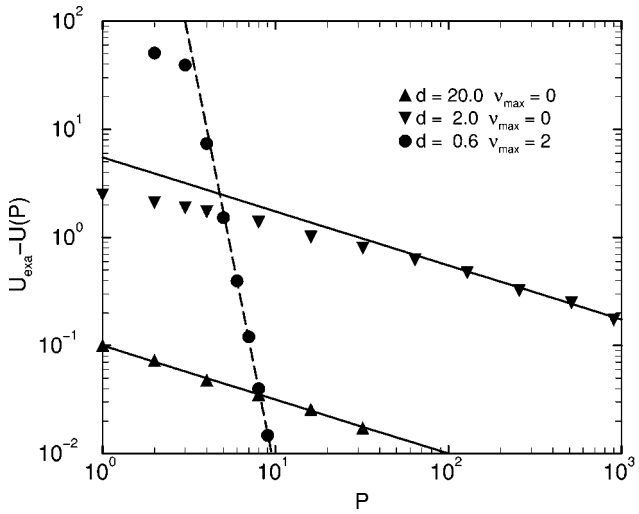


FIG. 1. Deviation of internal energy $U$ calculated with finite $P$ from exact results for different boxlengths $d$ and different numbers of periodic images $\nu_{\max}$ as a function of Trotter number; temperature $T=1$. Solid lines show $P^{-1/2}$, dashed line $P^{-8}$.

where $\lambda(\beta/P)$ is the thermal de Broglie wavelength at temperature $\tilde{T}=P/\beta k_B$.

In a simulation, e.g., of two or more interacting particles in a box, the free-particle propagator in the form of Eq. (12) can only be evaluated for finite $|\nu| \leqslant \nu_{\max}$. This is of course an approximation and it is convenient to call it an image approximation of degree $\nu_{\max}$. The image approximation of degree zero leads to the primitive algorithm, of course.

### B. Simulations

Although there is a variety of work using PIMC in conjunction with hard walls, a quantitative discussion of how fast the quantum limit is reached has yet to be given. We want to fill this gap by discussing three models: (i) Free particle in a box and primitive algorithm. (ii) Free particle in a box with image approximation of degree two. (iii) Well-behaved potentials in a box and image approximation of degree two. We note in passing that for odd values of $\nu_{\max}$ negative probabilities may occur, invoking the so-called sign problem and tedious averaging of observables. It is therefore convenient only to work with an even number $\nu_{\max}$. Although we treat only simple examples we see no obvious reason to call in question the generality of these results, as long as boundary conditions and potentials are well behaved.

All computations were done in a three-dimensional cubic box with boxlength $d$ at the dimensionless temperature $T=1$. We are thus dealing with the three-dimensional generalization of model Eq. (6). The quantity of interest is the internal energy or, in this case, the expectation value of the kinetic energy. The exact value of this quantity (in the quantum limit) can easily be calculated.

In Fig. 1, the following behavior is observed: In the primitive algorithm the error vanishes only proportionally to $P^{-1/2}$. At temperature $T=1$, the scaling behavior sets in at Trotter numbers as small as $P=1$ for the ''large'' box, $d=20$ (dimensionless units, $m=1$, $\hbar=1$). However, for the ''small'' box, $d=2$, one has to go to Trotter numbers as high as $P=100$ before the error shows $\langle U_{\text{exact}}(\beta)-U_P(\beta)\rangle \propto P^{-1/2}$. If, however, images are included, e.g., $\nu_{\max}=2$, the convergence goes $\propto P^{-8}$ as can be seen in Fig. 1, too.

For particles moving in a hard-wall box and interacting with each other through a continuous potential or with a continuous external potential the systematic quantum-discretization error vanishes again proportional to $P^{-2}$ as long as periodic images are taken into account. This is because all the arguments of the derivation[1] of Eq. (1) hold and terms that vanish faster than with $P^{-2}$ do not need to be taken into account in a $P^{-2}$–extrapolation.

It is important to note that taking into account higher-order images not only invokes results closer to the quantum limit but that in addition the *scaling behavior* sets in at smaller $P$ than if only low-order images are taken into account. This is the main merit of the use of periodic images.

The results presented in this section are presumably not only of interest for the system investigated here but also for problems such as quantum-interactions of hard spheres and one-dimensional rotators, where boundary conditions related to the ones discussed in this paper have to be respected. The use of images and knowing the convergence of the free-particle kernel with respect to Trotter number might also be important when fixed-node approximations are applied, which might be useful to treat fermions within the PIMC scheme.[14]

## III. COULOMB POTENTIAL

### A. Theory

As in the previous section, we first discuss the commutator defined in Eq. (8) for the Coulomb potential. To do so, however, we replace the Coulomb potential by the effective potential introduced in Eq. (4) and we assume that the damping radius $a$ is small in comparison to the Bohr radius $a_0$, or in atomic units $a \ll 1$. In this case it is possible to apply first-order perturbation theory and to obtain

$$\langle \psi_0|[T_{\text{kin}},V_{\text{eff}}]|\psi_0\rangle = -\frac{e^2\hbar^2}{2\pi\varepsilon_0 a m a_0^2}+\mathcal{O}(a^0). \tag{13}$$

Hence in the Coulombic limit, $a\to 0$, $\langle [T_{\text{kin}},V_{\text{eff}}]\rangle$ is not defined. It is an easy matter to see that the singularity proportional to $a^{-1}$ is not more severe if the bracket on the left-hand side of Eq. (13) is formed by any bounded eigenstate. Thus to leading order at finite temperatures,

$$\langle [T_{\text{kin}},V_{\text{eff}}]\rangle \propto a^{-1}. \tag{14}$$

This is an important result in order to estimate the leading difference between the partition function of the bare Coulomb problem in the quantum limit and the ''effective'' problem for finite $P$.

In addition to the Trotter extrapolation, $P\to\infty$, one has also to carry out a potential extrapolation $a\to 0$, see Eq. (4). Since in first order perturbation theory $\langle V_{\text{eff}}-V_C\rangle \propto a^2$ the leading error in the partition function is

$$Z_C(\beta)=Z_{\text{eff}}(\beta)+\mathcal{O}(a^2), \tag{15}$$

which can be shown by a cumulant expansion of the partition function. In Eq. (15), $Z_C(\beta)$ denotes the partition function for the Coulomb potential and $Z_{\text{eff}}(\beta)$ the one for the effective potential. With Eqs. (1), (14), (15) we obtain for $Z_C(\beta)$,

$$Z_C(\beta)=Z_{P,\text{eff}}(\beta)+\mathcal{O}(a^2)+\mathcal{O}\left(\frac{1}{a}P^{-2}\right). \tag{16}$$

This suggests that $a$ be made proportional to a power of $P$. The fastest convergence rate to the quantum and Coulomb potential limit in the primitive algorithm is obtained by taking

$$a\propto P^{-2/3}, \tag{17}$$

so that

$$Z_C(\beta)=Z_{P,\text{eff}}(\beta)+\mathcal{O}(P^{-4/3}). \tag{18}$$

Equation (17) together with Eq. (18) not only provides an efficient choice of the damping radius $a$ but also shows how to scale the Monte Carlo data at finite $P$ (and hence simultaneously $a$) to the Coulomb and the quantum limit. Note that this $P^{-4/3}$–convergence is even faster than the $P^{-1/2}$–convergence obtained if high-order approximants are employed without introducing an effective potential. In the next subsection we show that for suitable prefactors in Eq. (17) the convergence sets in at even much lower Trotter numbers than for the ''straight forward'' Takahashi Imada algorithm. Of course, a method which combines the Takahashi Imada algorithm, where for well-behaved potentials $Z(\beta)=Z_P(\beta)+\mathcal{O}(P^{-4})$, with the damped Coulomb potential method should give even faster convergence than $P^{-4/3}$. However, effectively three-body potentials[15] will then have to be calculated and we do not yet know the prefactor that must replace the term $1/a$ on the right-hand side of Eq. (18).

### B. Simulations

In this subsection we report simulation results based on the above interpolation scheme. Because the partition function for the Coulomb potential diverges, a cutoff in phase space or hard walls have to be introduced. For reasons of simplicity we chose a cubic box with boxlength $d=20$ (in atomic units). The positive charge is fixed in the center of the cubic box. We chose the temperature to be $T=0.02$ in atomic units so that the system will be groundstate dominated. Remember that the eigenenergies for the bare hydrogen problem in atomic units are $E_n=-0.5/n^2$, $n=1,2,\ldots,$ and the Bohr radius is $a_0=1$.

The radial distribution function $g(r)$, defined by

$$g(r)=\frac{1}{Z(\beta)}\int d^3r'\langle r'|\delta(r-r')e^{-\beta H}|r'\rangle, \tag{19}$$

for various Trotter numbers is plotted in Fig. 2. In addition we show the $(1s)$-radial distribution function, which corresponds to the exact solution for $T=0$ and $d=\infty$. The agreement between simulation and experiment becomes excellent for Trotter numbers $P>160$. See for comparison Fig. 7 in Ref. 7 (Takahashi Imada algorithm with bare Coulomb potential), where the $P=800$ compares to our $P=80$ curve.

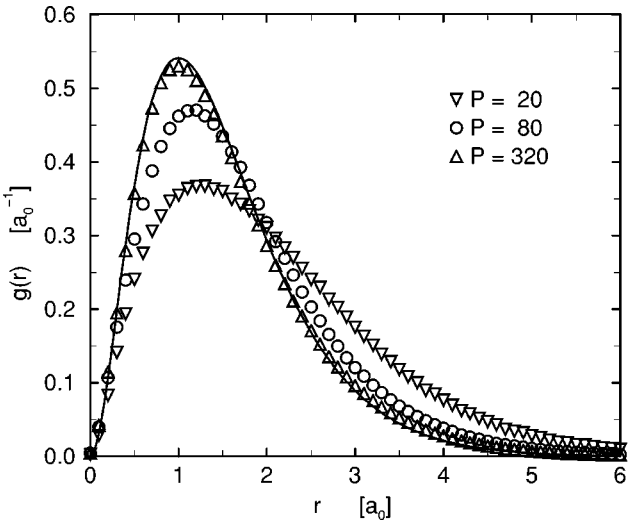


FIG. 2. Radial distribution function $g(r)$ of the hydrogen atom in a cubic box at $T=0.02$ for various Trotter numbers $P$ and damping radii $a=(TP)^{-2/3}$. The solid line corresponds to the $(1s)$ state.

In Fig. 3 the scaling with $P^{-4/3}$ of the internal energy is demonstrated. Two series of simulations are carried out, where the prefactor in Eq. (17) is chosen differently. As predicted by Eq. (18) the quantum-discretization error vanishes proportionally to $P^{-4/3}$. The values, where the scaling behavior starts, namely $P\approx 80$ for temperatures as low as $T=0.02$, are surprisingly small. The (groundstate dominated) energy $E=-0.487$ is larger than the real groundstate of $E_1=-0.5$ because of the hard-wall boundary condition. For the present choice of temperature and boundary conditions the deviation is invoked by the kinetic energy term, since the ''box-restricted'' groundstate is more localized than in the $d=\infty$ case. If we took a much larger simulation box than in the present example (without changing the temperature) a

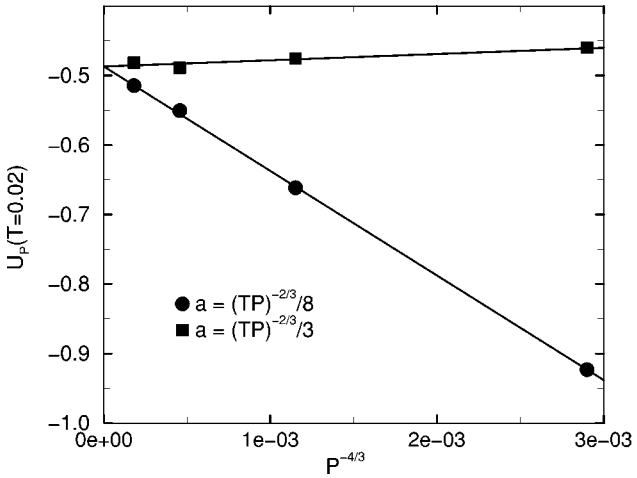


FIG. 3. Internal energy $U$ of the hydrogen atom in a cubic box as a function of Trotter number $P$ at temperature $T=0.02$ for different prefactors for the damping radius $a$; see Eq. (17). Lines are drawn to guide the eye.

deviation from $E_1$ would be obtained due to finite-temperature dissociation.

In passing we want to note that it would have been an easy matter to include the motion from the proton out of the center of the box. However, this procedure does not include new principles and makes the comparison to exact results more difficult.

## IV. CONCLUSIONS

In this paper we deal with two problems that are pathological for the primitive path-integral Monte Carlo (PIMC) formalism, hard walls and the Coulomb potential. A simple strategy for circumventing the strong pathology of the Coulomb potential is suggested. It is shown that this startegy works so well that we expect it to be useful for simulating many problems hitherto not accessible to path-integral simulations.

## ACKNOWLEDGMENTS

M.H.M. gratefully acknowledges a Feodor Lynen Fellowship of the Alexander Humboldt Foundation. This work was supported by a grant to B.J.B. from the National Science Foundation.

[1] M. Suzuki, in *Quantum Monte Carlo Methods in Equilibrium and Non-equilibrium Systems*, Springer Series in Solid-State Sciences, edited by M. Suzuki (Springer, Berlin, 1986), Vol. 74.
[2] J. A. Barker, J. Chem. Phys. **70**, 2914 (1979).
[3] G. Jacucci and E. Omerti, J. Chem. Phys. **76**, 2382 (1983).
[4] S. V. Lawande, C. A. Jensen, and H. L. Sahlin, J. Comput. Phys. **3**, 416 (1969).
[5] H. De Raedt and B. De Raedt, Phys. Rev. A **28**, 3575 (1983).
[6] M. Takahashi and M. Imada, J. Phys. Soc. Jpn. **53**, 3765 (1984).
[7] X.-P. Li and J. Q. Broughton, J. Chem. Phys. **86**, 5094 (1987).
[8] Z.-H. Liu and J. Broughton, Phys. Rev. B **40**, 571 (1989).
[9] C. Pierleoni, D. M. Ceperley, B. Bernu, and W. R. Magro, Phys. Rev. Lett. **73**, 2145 (1994).
[10] The partition function of the hydrogen potential is not defined, of course. We have in mind a system where the proton is constrained to the center of a spherical (cubic) unpenetrable cavity, whose diameter (boxlength) $d$ is so large that the groundstate energy is effected only very little, e.g., $d=20a_0$.
[11] S. Sorella, S. Baroni, R. Car, and M. Parrinello, Europhys. Lett. **8**, 663 (1989).
[12] E. Y. Loh, Jr., J. E. Gubernatis, R. T. Scalettar, S. R. White, D. J. Scalapino, and R. L. Sugar, Phys. Rev. B **41**, 9301 (1990).
[13] The partition function of a particle in a box with finite walls is not defined, of course. We have in mind a system which is periodically repeated and whose spacing between different basins is so large that the groundstate energy is affected only very little.
[14] D. M. Ceperley, J. Stat. Phys. **63**, 1237 (1991); D. F. B. ten Haaf, H. J. M. van Bemmel, D. M. Ceperley, Phys. Rev. B **51**, 13 039 (1995).
[15] In the Takahashi Imada algorithm the *total* force acting on each particle enters the effective potential. Hence the potential can not be written as a sum over two-body interactions.